

# Parts per trillion sensitivity for ethane in air with an optical parametric oscillator cavity leak-out spectrometer

Golo von Basum, Daniel Halmer, Peter Hering, and Manfred Mürtz

*Institut für Lasermedizin, Universität Düsseldorf, Universitätsstrasse 1, D-40225 Düsseldorf, Germany*

Stephan Schiller

*Institut für Experimentalphysik, Universität Düsseldorf, Universitätsstrasse 1, D-40225 Düsseldorf, Germany*

Frank Müller, Alexander Popp, and Frank Kühnemann

*Institut für Angewandte Physik, Universität Bonn, Wegelerstrasse 8, D-53115 Bonn, Germany*

Received October 16, 2003

Spectroscopic detection of ethane in the 3- $\mu\text{m}$  wavelength region was performed by means of a cw optical parametric oscillator and cavity leak-out. We achieved a minimum detectable absorption coefficient of  $1.6 \times 10^{-10} \text{ cm}^{-1}/\sqrt{\text{Hz}}$ , corresponding to an ethane detection limit of 6 parts per trillion/ $\sqrt{\text{Hz}}$ . For 3-min integration time the detection limit was 0.5 parts per trillion. The levels are to our knowledge the best demonstrated so far. These frequency-tuning capabilities facilitated multigas analysis with simultaneous monitoring of ethane, methane, and water vapor in human breath. © 2004 Optical Society of America

OCIS codes: 300.6340, 300.6360, 300.1030, 140.3580.

The quantitative analysis of trace gases in ambient air is of considerable interest for a number of applications, such as environmental monitoring and medical breath tests. For these tasks, mobile analyzers with high sensitivity, specificity, and speed are required. Several high-resolution mid-infrared ( $\lambda = 3\text{--}20 \mu\text{m}$ ) spectroscopy techniques, e.g., photoacoustic spectroscopy,<sup>1,2</sup> Faraday modulation spectroscopy,<sup>3</sup> cavity ring-down spectroscopy,<sup>4</sup> and cavity leak-out spectroscopy (CALOS), which is a cw variant of cavity ring-down spectroscopy,<sup>5</sup> have been reported to provide detection sensitivities on the sub-parts-in- $10^9$  (ppb) level. For example, the present authors and colleagues previously demonstrated that CALOS is advantageous for sensitive and specific analysis of ethane in exhaled human breath.<sup>6</sup> The implementation of all these techniques as transportable trace-gas detectors strongly relies on the development of suitable all-solid-state mid-infrared laser light sources to provide narrow linewidth and wide tunability at sufficient power levels. To this end, nonlinear frequency-conversion devices [i.e., difference-frequency generators and optical parametric oscillators (OPOs)] and the recently developed quantum cascade lasers are currently under investigation.<sup>1,7</sup> We recently reported what is to our knowledge the first CALOS trace-gas measurements based on a cw OPO. This OPO used a common-cavity pump-resonant, singly resonant setup<sup>8</sup> and had the advantages of higher mid-infrared output power than difference-frequency generation devices and lower pump power levels than ordinary singly resonant OPOs. A drawback of this common-cavity pump-resonant design, however, was the limitation of its frequency tunability, which hindered exact targeting at the maxima of absorption lines. Here we present a novel setup that in contrast to the former utilizes a pump-resonant singly resonant oscillator with two independent cavities.<sup>9</sup> The separation of signal and

pump wave cavities results in significantly improved frequency-tuning characteristics. Thereby it has become possible to freely choose those frequencies in the molecular spectrum that optimize the CALOS signal and selectivity. Furthermore, the careful implementation of data acquisition and analysis considerably reduces the baseline noise level. To demonstrate the improved tuning behavior and overall performance of this new detector we carried out ethane measurements in exhaled human breath. Ethane monitoring on the sub-ppb level is of considerable interest for medical diagnostics because increased breath ethane is considered a reliable indicator of increased damage by reactive oxygen species in an organism. Furthermore, we demonstrate a multigas analysis that requires no pretreatment of the exhaled gas.

The experimental setup consists of a cw OPO, an acousto-optic modulator (AOM), an absorption cell (CALOS cell), and a fast photodetector (Fig. 1). The OPO is used to excite a fundamental transverse mode ( $\text{TEM}_{00}$ ) of the CALOS cell, a high-finesse optical resonator ( $L = 52.5 \text{ cm}$ ) formed by two highly reflective mirrors ( $R = 99.985\%$ ), as previously described by Kleine *et al.*<sup>10</sup> We determine absorption coefficients of the analyzed gas samples by measuring the decay time of the CALOS cell after the exciting radiation is turned off.

The OPO was originally developed for the requirements of a transportable photoacoustic spectrometer.<sup>11</sup> A cw pump-resonant singly resonant oscillator<sup>9,12</sup> (PR-SRO) is set up in a linear dual-cavity design and uses a heated periodically poled lithium niobate<sup>13</sup> (PPLN) crystal as a nonlinear medium (length, 19 mm; width, 50 mm; thickness, 0.5 mm). The front surface of the PPLN crystal is high-reflection coated for the pump and signal waves ( $R_{\text{pump}} = 94.3\%$ ;  $R_{\text{signal}} = 99.9\%$ ; rear surface, antireflection coated). The pump cavity is closed by a meniscus mirror ( $R_{\text{pump}} = 99.9\%$ ,  $R_{\text{signal}} < 2\%$ ,

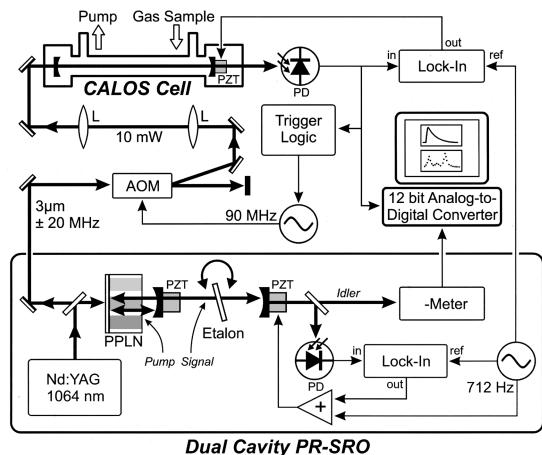


Fig. 1. Schematic of the experimental setup: Ls, lenses; PDs, photodetectors; other abbreviations defined in text.

$R_{\text{idler}} < 5\%$ ); the signal cavity, by a concave mirror ( $R_{\text{signal}} = 99.9\%$ ,  $R_{\text{idler}} < 5\%$ ). Both mirrors are attached to piezoceramic transducers (PZTs) to adjust cavity lengths. All optics are antireflection coated for the idler wavelength. A galvanometer-mounted etalon ( $R = 50\%$ ,  $d = 0.5$  mm) inside the signal cavity suppresses spontaneous mode hops and can be used for mode-hop frequency tuning. Idler frequency tuning is performed in any of five ways: (1) coarse tuning from 3.1 to 3.9  $\mu\text{m}$  by selecting one of the 19 crystal gratings ( $\Lambda = 28.64\text{--}30.16$   $\mu\text{m}$ ) by use of a motor-driven translation stage, (2) temperature tuning of the PPLN from 150 to 200  $^{\circ}\text{C}$ , (3) 450-MHz-steps mode-hop tuning (52-GHz working range) by turning the etalon with the galvanometer, (4) continuous fine tuning over 450 MHz by changing the signal cavity length, (5) fine tuning (up to 1.5 GHz mode-hop free; 40 GHz in total) by tuning the pump laser (Nd:YAG;  $\lambda = 1064$  nm; linewidth,  $\approx 1$  kHz in 100 ms;  $P = 2.5$  W). Idler output power is as much as 100 mW at each end of the OPO.

The pump cavity is locked to the laser by use of a Pound–Drever–Hall scheme. The length of the signal cavity can be modulated without affecting the pump cavity stabilization. This results in a frequency modulation of signal and idler waves that is used to frequency stabilize the signal cavity to the maximum of the OPO gain curve by means of a  $1f$  lock-in technique. The frequency of the idler wave is measured with a mid-infrared wavemeter. The frequency stability is better than the  $\pm 30$ -MHz accuracy of the wavemeter in a period of 45 min.

The idler beam ( $\text{Ge}$ ;  $f_{\text{mod}} = 90$  MHz) is focused into the AOM that forms a rapidly switchable 90-MHz frequency-shifted beam. This deflected beam is matched to the  $\text{TEM}_{00}$  mode of the CALOS cell by means of two lenses. Because the idler frequency is modulated, the CALOS cell is periodically excited. Moreover, we use this modulation to lock a single  $\text{TEM}_{00}$  cavity mode to the OPO by adjusting the length of the CALOS cell. When the transmitted intensity exceeds a certain threshold, a trigger pulse is released, which shuts off the AOM. The subsequent decay of the cavity field is monitored by the photodetector and

transferred to a 12-bit analog-to-digital conversion card in the control computer. We determine the decay time of the leak-out signal by fitting a single exponential to the data. We achieved a data acquisition rate of 1.4 kHz, corresponding to a modulation frequency of the signal cavity of 700 Hz. By measuring the decay time of the empty cell ( $\tau_0$ ) as well as the decay time of the cell filled with the gas sample ( $\tau$ ) we can determine the absolute absorption coefficient ( $\alpha$ ) by  $\alpha = 1/c \times (1/\tau - 1/\tau_0)$ , where  $c$  is the speed of light.

For the most sensitive and selective detection of ethane the OPO was tuned to the strongest absorption of ethane at a pressure of 100 hPa, which is located at  $2983.38$   $\text{cm}^{-1}$  according to Fourier-transform infrared spectroscopy (FTIR) measurements. The observed spectrum for an ethane concentration of 21.5 ppb is shown in Fig. 2A. Pivotal criteria for sensitive detection are the magnitude and the stability of the measured decay time in the absence of absorption. Using grade 5 nitrogen as a nonabsorbing gas yields a standard error of the mean value of the absorption coefficient of  $\sigma_m = 1.6 \times 10^{-10}$   $\text{cm}^{-1}/\sqrt{\text{Hz}}$  (Fig. 2B). The good frequency stability of the OPO permits averaging for as long as 180 s, resulting in a noise equivalent absorption of  $1.2 \times 10^{-11}$   $\text{cm}^{-1}$ . To test the performance of the OPO–CALOS setup we prepared different concentrations of ethane. Using two mass-flow controllers, we mixed grade 5 nitrogen with a certified gas mixture of 1 part in  $10^6$  (ppm) of ethane in nitrogen to obtain concentrations of 100 to 4 ppb. The smallest mixing ratio is limited by the error of the mass-flow controllers (1% of maximum value). To obtain even smaller concentrations, of 2 to 0.04 ppb, we mixed ambient air containing 2.26 ppb of ethane (measured with CALOS) with grade 5 nitrogen. For this measurement the sample gas was cleaned by means of a cooling trap ( $T = 115$  K) placed between the mass-flow controller and the CALOS cell. This trap is used to eliminate any disturbing molecules (e.g., water) from the gas

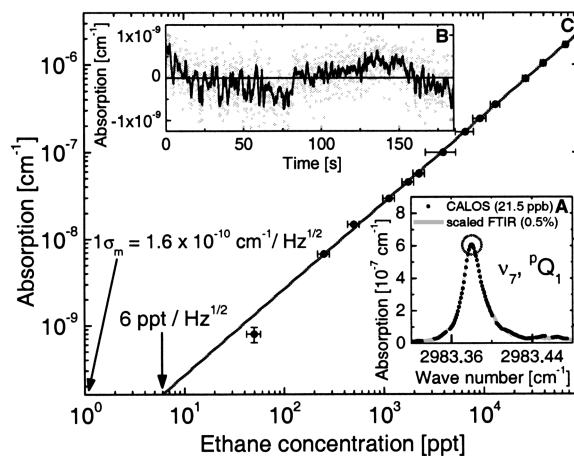


Fig. 2. A, measured spectrum of 21.5-ppb ethane in  $\text{N}_2$  at a pressure of 100 hPa. B, Background noise of the OPO CALOS setup, revealing a noise equivalent absorption of  $1\sigma_m = 1.6 \times 10^{-10}$   $\text{cm}^{-1}/\sqrt{\text{Hz}}$ . C, Measured absorption versus ethane concentration. The noise-equivalent ethane concentration is 6 ppt/ $\sqrt{\text{Hz}}$ . The line is a linear fit.

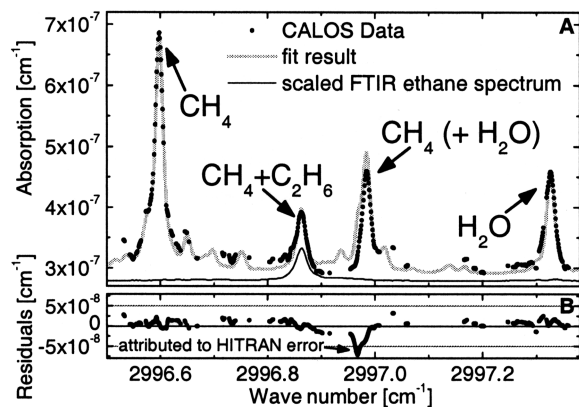


Fig. 3. A, CALOS spectrum obtained from a breath sample and calculated spectrum; B, residuals between data and fit.

sample. Figure 2C depicts the measured absorption coefficient at the peak of the ethane absorption line as a function of concentration. The abscissa crosses the ordinate at the noise level of our setup. The diagram reveals a detection limit (signal/noise ratio of 1) of 6 parts in  $10^{12}$  (ppt)/ $\sqrt{\text{Hz}}$  of ethane, which to our knowledge is unprecedented.

The frequency tunability of the OPO allows one to select a spectral region for the analysis of ethane without significant interference from other gases. Thus no cooling trap or other sample preparation is required. The optimum spectral region ranges from 2996.5 to 2997.4  $\text{cm}^{-1}$ . To study the performance of the OPO-CALOS setup we analyzed a breath sample from a volunteer. The breath was collected in a sample bag made from Tedlar that was then connected to the inlet of the flowmeter (flow, 50 cubic centimeters per minute at STP). Figure 3 depicts the measured data of the breath sample. The spectrum reveals four absorption structures, which belong to ethane, methane, and water. Other substances (e.g., isoprene, acetone) that are present in human breath show spectrally flat absorption within this spectral range. To determine the concentrations of the three molecular species and the flat background we applied a four-parameter linear regression (least-squares fit). We used the Hitran database<sup>14</sup> to obtain the spectra of  $\text{CH}_4$  and  $\text{H}_2\text{O}$ , and a FTIR spectrum for  $\text{C}_2\text{H}_6$ . The irregularity near 2996.97  $\text{cm}^{-1}$  is attributed to an error of the water spectrum from the Hitran database. The analyzed breath sample contained  $(10.8 \pm 0.5)$  ppm methane,  $(2.4 \pm 0.5)$  ppb ethane, and  $(2.1 \pm 0.2)\%$  water. The constant offset was  $(27.9 \pm 0.1) \times 10^{-8} \text{ cm}^{-1}$ . The water concentration agrees with the concentration of saturated water vapor at a temperature of 20 °C (2.3%). The amount of breath ethane was close to the ambient air concentration of  $(2.7 \pm 0.5)$  ppb, which was measured directly before the breath sampling. The ambient air concentration of methane was  $(1.9 \pm 0.5)$  ppm, and

therefore the volunteer had exhaled  $(7.9 \pm 0.7)$  ppm of methane.

We have reported a CALOS setup with a dual-cavity PR-SRO as the mid-infrared cw light source featuring excellent tuning characteristics. This enhanced frequency tunability, together with improvements in signal acquisition and processing, allows an unprecedentedly low (sub-ppt) detection limit for ethane. This is ten times better than from other high-sensitivity ethane detection setups.<sup>1</sup> Furthermore, the simultaneous detection of several gases is possible, as we demonstrated by measuring ethane, methane, and water in human breath, without the need for any pretreatment. The reported setup has a high potential for use as a transportable, all-solid-state ultrasensitive trace-gas analyzer for environmental and medical studies.

This research is part of the Ph.D. dissertation of G. von Basum at the Faculty of Mathematics and Science, Heinrich-Heine Universität, Düsseldorf, Germany. It was financially supported by the Deutsche Forschungsgemeinschaft. M. Mürtz's e-mail address is muertz@uni-duesseldorf.de.

## References

1. M. M. J. W. van Herpen, S. C. Li, S. E. Bisson, and F. J. M. Harren, *Appl. Phys. Lett.* **81**, 1157 (2002).
2. F. Kühnemann, K. Schneider, A. Hecker, A. A. E. Martis, W. Urban, S. Schiller, and J. Mlynek, *Appl. Phys. B* **66**, 741 (1998).
3. H. Ganser, W. Urban, and A. M. Brown, *Mol. Phys.* **101**, 545 (2003).
4. J. J. Scherer, D. Voelkel, D. J. Rakestraw, J. B. Paul, C. P. Collier, R. J. Saykally, and A. O'Keefe, *Chem. Phys. Lett.* **245**, 273 (1995).
5. B. A. Paldus, C. C. Harb, T. G. Spence, R. N. Zare, C. Gmachl, F. Capasso, D. L. Sivco, J. N. Baillargeon, A. L. Hutchinson, and A. Y. Cho, *Opt. Lett.* **25**, 666 (2000).
6. G. von Basum, H. Dahnke, D. Halmer, P. Hering, and M. Mürtz, *J. Appl. Physiol.* **95**, 2583 (2003).
7. D. Richter, A. Fried, B. P. Wert, J. G. Walega, and F. K. Tittel, *Appl. Phys. B* **75**, 281 (2002).
8. A. Popp, F. Müller, F. Kühnemann, S. Schiller, G. von Basum, H. Dahnke, P. Hering, and M. Mürtz, *Appl. Phys. B* **75**, 751 (2002).
9. G. A. Turnbull, D. McGloin, I. D. Lindsay, M. Ebrahimzadeh, and M. H. Dunn, *Opt. Lett.* **25**, 341 (2000).
10. D. Kleine, H. Dahnke, W. Urban, P. Hering, and M. Mürtz, *Opt. Lett.* **25**, 1606 (2000).
11. F. Müller, A. Popp, F. Kühnemann, and S. Schiller, *Opt. Express* **11**, 2820 (2003), <http://www.opticsexpress.org>.
12. K. Schneider, P. Kramer, S. Schiller, and J. Mlynek, *Opt. Lett.* **22**, 1293 (1997).
13. L. E. Myers, R. C. Eckardt, M. M. Fejer, R. L. Byer, and W. R. Bosenberg, *Opt. Lett.* **21**, 591 (1996).
14. Hitran2000 spectral database, <http://www.hitran.com>.